

Exact Out-of-Time-Ordered Correlation Functions for an Interacting Lattice Fermion Model

Naoto Tsuji,¹ Philipp Werner,² and Masahito Ueda^{1,3}

¹RIKEN Center for Emergent Matter Science (CEMS), Wako 351-0198, Japan

²Department of Physics, University of Fribourg, 1700 Fribourg, Switzerland

³Department of Physics, University of Tokyo, Hongo, Tokyo 113-0033, Japan

(Dated: November 13, 2018)

Exact solutions for local equilibrium and nonequilibrium out-of-time-ordered correlation (OTOC) functions are obtained for a lattice fermion model with on-site interactions, namely the Falicov-Kimball (FK) model, in the large dimensional and thermodynamic limit. Our approach is based on the nonequilibrium dynamical mean-field theory generalized to an extended Kadanoff-Baym contour. We find that the density-density OTOC is most enhanced at intermediate coupling around the metal-insulator phase transition. In the high-temperature limit, the OTOC remains nontrivially finite and interaction-dependent, even though dynamical charge correlations probed by an ordinary response function are completely suppressed. We propose an experiment to measure OTOCs of fermionic lattice systems including the FK and Hubbard models in ultracold atomic systems.

There is a growing interest in the scrambling and spreading of information in quantum many-body systems in wide areas of physics ranging from condensed matter to black holes [1–22]. A useful measure to diagnose the sensitivity of time-evolving quantities on the initial condition is the out-of-time-ordered correlation (OTOC) function [23] of two operators W and V ,

$$C(t) = -\langle [W(t), V(0)]^2 \rangle. \quad (1)$$

In the semiclassical picture, if we choose $W = p_j, V = p_k$, $C(t) \sim \langle (\partial p_j(t)/\partial q_k(0))^2 \rangle$ (p_j and q_k are canonical momenta and coordinates), so that OTOCs reflect how the system is scrambled and the initial-condition dependence is amplified. In chaotic systems, OTOCs are expected to grow exponentially in time (butterfly effect). It has been conjectured based on the holographic principle that there is a universal bound for the exponential growth rate of OTOCs (Lyapunov exponent) [9]. Recently, the OTOC has been analytically evaluated for the Sachdev-Ye-Kitaev (SYK) model, a model of fermions having all-to-all four-body random interactions without hopping [6, 24–28]. It was found to show exactly such a chaotic behavior with the bound saturated [6].

An immediate question is how OTOCs grow in the lattice fermion models with short-range interactions that are typically used to describe strongly correlated condensed matter systems. To evaluate Eq. (1), one needs to compute quantities like $\langle W(t)V(0)W(t)V(0) \rangle$, which are incompatible with the usual time-ordered sequence of operators on the Keldysh or Kadanoff-Baym contour \mathcal{C} ($0 \rightarrow t \rightarrow 0 \rightarrow -i\beta$, β is the initial inverse temperature) [29–31]. This is in contrast to ordinary response functions. For example, a nonlinear optical susceptibility is given by a combination of current correlators such as $\langle [j(t), j(t')], [j(t''), j(t''')] \rangle$ with a causality constraint $t \geq t' \geq t'' \geq t'''$ [32], which can always be defined on \mathcal{C} . Due to the unconventional ordering, OTOCs have not been much studied for correlated lattice fermion models. Up to now, OTOC functions have been calculated mostly by exact diagonalization for spin [10, 13–15, 19] and boson [16] systems of small size.

In this Letter, we generalize the nonequilibrium dynamical

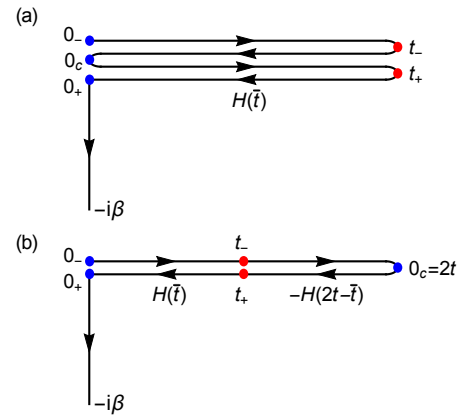


FIG. 1. Two types of extended [doubly folded (a) and singly folded (b)] Kadanoff-Baym contours $\tilde{\mathcal{C}}$, which are equivalent. In (a), the system evolves with the Hamiltonian $H(\bar{t})$ ($0 \leq \bar{t} \leq t$), while in (b) the system evolves with $H(\bar{t})$ for $0 \leq \bar{t} \leq t$ and $-H(2t - \bar{t})$ for $t \leq \bar{t} \leq 2t$.

mean-field theory (DMFT) [33, 34] to an extended Kadanoff-Baym contour, which allows one to calculate OTOC functions for lattice fermion models in the infinite-dimensional and thermodynamic limit. We apply this technique to the Falicov-Kimball (FK) model [35, 36], which admits an exact solution due to infinitely many conserved quantities. The FK model exhibits intriguing properties such as a metal-insulator transition, non-Fermi liquid behavior [36], and Anderson localization in two dimensions [37]. Its nonequilibrium aspects have also been studied [33, 38–43]. We show that OTOCs provide yet another insight into physics of this model, that cannot be obtained from ordinary response functions. Finally, we propose an experimental scheme with ultracold atoms to measure OTOCs in a fermion model.

We begin by noting that an out-of-time-ordered function $\langle W(t)V(0)W(t)V(0) \rangle$ is rewritten as

$$\frac{\text{Tr}[e^{-\beta H(0)} \mathcal{U}(0, t) W \mathcal{U}(t, 0) V \mathcal{U}(0, t) W \mathcal{U}(t, 0) V]}{\text{Tr}[e^{-\beta H(0)}]}$$

$$= \frac{\text{Tr}[\mathcal{T}_{\tilde{\mathcal{C}}} e^{-i \int_{\tilde{\mathcal{C}}} dt H(t)} W_{t_+} V_{0_c} W_{t_-} V_{0_-}]}{\text{Tr}[\mathcal{T}_{\tilde{\mathcal{C}}} e^{-i \int_{\tilde{\mathcal{C}}} dt H(t)}]} \equiv \langle \mathcal{T}_{\tilde{\mathcal{C}}} W_{t_+} V_{0_c} W_{t_-} V_{0_-} \rangle,$$

where $\mathcal{U}(t, t')$ is the unitary evolution operator, $\tilde{\mathcal{C}}$ is a doubly folded Kadanoff-Baym contour with time running as $0 (\equiv 0_-) \rightarrow t (\equiv t_-) \rightarrow 0 (\equiv 0_c) \rightarrow t (\equiv t_+) \rightarrow 0 (\equiv 0_+) \rightarrow -i\beta$ [see Fig. 1(a)] [44], and $\mathcal{T}_{\tilde{\mathcal{C}}}$ is the time ordering operator along $\tilde{\mathcal{C}}$. We can also unfold the contour $\tilde{\mathcal{C}}$ as shown in Fig. 1(b), where time runs as $0 \rightarrow 2t \rightarrow 0 \rightarrow -i\beta$. From t to $2t$, the time evolution is reversed, i.e., the system evolves with the Hamiltonian $-H(2t - \bar{t})$ ($t \leq \bar{t} \leq 2t$). These two types of contours are equivalent. It is straightforward to extend a field theory from \mathcal{C} to $\tilde{\mathcal{C}}$. The nonequilibrium Green's function is defined on $\tilde{\mathcal{C}}$ as $G(t, t') = -i \langle \mathcal{T}_{\tilde{\mathcal{C}}} c(t) c^\dagger(t') \rangle$ [c (c^\dagger) is the fermion annihilation (creation) operator]. By replacing \mathcal{C} with $\tilde{\mathcal{C}}$, the nonequilibrium DMFT is generalized as explicitly constructed below.

We consider the FK model with the Hamiltonian

$$H(t) = \sum_{ij} J_{ij} c_i^\dagger c_j + \sum_i (-\mu n_i^c + E_f n_i^f) + U(t) \sum_i n_i^f n_i^c, \quad (2)$$

where $n_i^c \equiv c_i^\dagger c_i$, $n_i^f \equiv f_i^\dagger f_i$, J_{ij} and μ are the hopping amplitude and the chemical potential for the c particles, E_f is the energy level for the f particles, and $U(t)$ is the on-site interaction, which can be time dependent. The model is exactly solvable in any dimension in the sense that $[H, n_i^f] = 0$ for all i , i.e., it has infinitely many conserved quantities. The immobile f particles act as a random potential for the itinerant c particles.

In the infinite dimensional limit ($d \rightarrow \infty$) with the hopping scaled as $J_{ij} \propto J_*/\sqrt{d}$ (J_* is a fixed constant) [45], the lattice model can be exactly mapped onto an impurity problem with a self-consistently determined dynamical mean field (hybridization function) $\Delta(t, t')$ [36, 46–49], where the action is given by

$$\begin{aligned} \mathcal{S}_{\text{imp}} = & \int_{\tilde{\mathcal{C}}} dt dt' c^\dagger(t) \Delta(t, t') c(t') \\ & + \int_{\tilde{\mathcal{C}}} dt [-\mu n^c(t) + E_f n^f(t) + U(t) n^f(t) n^c(t)]. \end{aligned} \quad (3)$$

The mapping is constructed such that the local lattice Green's function is equal to the impurity Green's function. In the large- d limit, the lattice self-energy becomes local and can be identified with the impurity self-energy. The single-particle Green's function for the FK model can be expressed as

$$G(t, t') \equiv -i \langle \mathcal{T}_{\tilde{\mathcal{C}}} c(t) c^\dagger(t') \rangle_{\mathcal{S}_{\text{imp}}} = \sum_{\alpha} w_{\alpha} R_{\alpha}(t, t'), \quad (4)$$

where $\alpha = 0$ and 1 correspond to empty and occupied f particle configurations, $w_1 = \langle n^f \rangle$, $w_0 = 1 - w_1$, and $R_{\alpha}(t, t')$ is a configuration-dependent Green's function, which satisfies the Dyson equation,

$$[i\partial_t + \mu - U(t)\alpha] R_{\alpha}(t, t') - \int_{\tilde{\mathcal{C}}} d\bar{t} \Delta(t, \bar{t}) R_{\alpha}(\bar{t}, t') = \delta_{\tilde{\mathcal{C}}}(t, t'). \quad (5)$$

Here the integral is taken along the contour $\tilde{\mathcal{C}}$, and $\delta_{\tilde{\mathcal{C}}}(t, t')$ is the generalized contour delta function [50]. $R_0(t, t')$ is the usual Weiss Green's function in the nonequilibrium DMFT [34]. Throughout this Letter, we consider the half-filled case (i.e., $\mu = U/2, w_1 = 0.5$) on the Bethe lattice with infinite coordinations, with the density of states $D(\epsilon) = \sqrt{4J_*^2 - \epsilon^2}/(2\pi J_*^2)$, and use J_* (J_*^{-1}) as the unit of energy (time). In this case, $\Delta(t, t')$ is related to the local Green's function via $\Delta(t, t') = J_*^2 G(t, t')$ [49]. Within DMFT, the model shows a metal-to-Mott insulator transition at $U = 2$, and the metallic phase is a non-Fermi liquid [36].

In the FK model, the impurity action (3) can be block-diagonalized into f -particle configuration sectors ($\alpha = 0, 1$), in which the c particles behave as free fermions in an effective potential $U(t)\alpha - \mu$. This makes it possible to calculate arbitrary local dynamical correlation functions exactly. Let us look at the 2-point charge correlation function, which is given by the sum of contributions from the two sectors,

$$C_2(t_1, t_2) \equiv \langle \mathcal{T}_{\tilde{\mathcal{C}}} n^c(t_1) n^c(t_2) \rangle = \sum_{\alpha} w_{\alpha} \langle \mathcal{T}_{\tilde{\mathcal{C}}} n^c(t_1) n^c(t_2) \rangle_{\mathcal{S}_{\text{imp}}^{\alpha}}, \quad (6)$$

where $\mathcal{S}_{\text{imp}}^{\alpha} = \int_{\tilde{\mathcal{C}}} dt dt' c^\dagger(t) \Delta(t, t') c(t') + \int_{\tilde{\mathcal{C}}} dt [U(t)\alpha - \mu] c^\dagger(t) c(t)$ is the sector α ($n^f = \alpha$) of the impurity action. Since $\mathcal{S}_{\text{imp}}^{\alpha}$ is quadratic with respect to the c -particle operators, we can analytically evaluate the right-hand side of Eq. (6) by Wick's theorem [51]. The result is

$$C_2(t_1, t_2) = \sum_{\alpha} w_{\alpha} [R_{\alpha}(t_1, t_2) R_{\alpha}(t_2, t_1) - R_{\alpha}(t_1, t_1) R_{\alpha}(t_2, t_2)]. \quad (7)$$

Here $R_{\alpha}(t, t')$ at equal times ($t = t'$) should be read as a lesser component (i.e., $t' = t + 0$). Equation (7) is symmetric with respect to the exchange $t_1 \leftrightarrow t_2$, and satisfies the boundary condition $\lim_{t_2 \rightarrow t_1} C_2(t_1, t_2) = \langle n^c(t_1) \rangle$.

As shown in [52], Eq. (7) correctly reproduces the previous result for the dynamical charge susceptibility [36, 53–55]

$$\chi(t, t') = i\theta(t - t') \langle [n^c(t), n^c(t')] \rangle. \quad (8)$$

In the infinite dimensional limit, the local dynamical charge susceptibility is equal to the lattice charge susceptibility $\chi_{\mathbf{q}}(t, t')$ at general momentum \mathbf{q} (randomly chosen from the Brillouine zone), since $\chi(t, t') = N_{\mathbf{q}}^{-1} \sum_{\mathbf{q}} \chi_{\mathbf{q}}(t, t')$ and general momenta \mathbf{q} make equal and dominant contributions to the momentum sum. In fact, we can confirm by explicit calculations that expression (7) gives the correct dynamical charge susceptibility for general momentum [52].

The calculation can straightforwardly be generalized to arbitrary n -point local charge correlation functions. The 3-point

function is given by

$$\begin{aligned}
C_3(t_1, t_2, t_3) &\equiv \langle \mathcal{T}_{\tilde{C}} n^c(t_1) n^c(t_2) n^c(t_3) \rangle \\
&= \sum_{\alpha} w_{\alpha} \{ i[R_{\alpha}(t_1, t_2) R_{\alpha}(t_2, t_3) R_{\alpha}(t_3, t_1) + (1 \text{ term})] \\
&\quad - i[R_{\alpha}(t_1, t_1) R_{\alpha}(t_2, t_3) R_{\alpha}(t_3, t_2) + (2 \text{ terms})] \\
&\quad + iR_{\alpha}(t_1, t_1) R_{\alpha}(t_2, t_2) R_{\alpha}(t_3, t_3) \}, \tag{9}
\end{aligned}$$

and the 4-point function by

$$\begin{aligned}
C_4(t_1, t_2, t_3, t_4) &\equiv \langle \mathcal{T}_{\tilde{C}} n^c(t_1) n^c(t_2) n^c(t_3) n^c(t_4) \rangle \\
&= \sum_{\alpha} w_{\alpha} \{ -[R_{\alpha}(t_1, t_2) R_{\alpha}(t_2, t_3) R_{\alpha}(t_3, t_4) R_{\alpha}(t_4, t_1) + (5 \text{ terms})] \\
&\quad + [R_{\alpha}(t_1, t_1) R_{\alpha}(t_2, t_3) R_{\alpha}(t_3, t_4) R_{\alpha}(t_4, t_2) + (7 \text{ terms})] \\
&\quad - [R_{\alpha}(t_1, t_1) R_{\alpha}(t_2, t_2) R_{\alpha}(t_3, t_4) R_{\alpha}(t_4, t_3) + (5 \text{ terms})] \\
&\quad + [R_{\alpha}(t_1, t_2) R_{\alpha}(t_2, t_1) R_{\alpha}(t_3, t_4) R_{\alpha}(t_4, t_3) + (2 \text{ terms})] \\
&\quad + R_{\alpha}(t_1, t_1) R_{\alpha}(t_2, t_2) R_{\alpha}(t_3, t_3) R_{\alpha}(t_4, t_4) \}. \tag{10}
\end{aligned}$$

In Eqs. (9) and (10), we group the terms by topologically equivalent Wick contractions, and in each group one representative term is spelt out. As a consistency check, one can see that the right-hand sides of Eqs. (9) and (10) are invariant under arbitrary permutations $t_i \leftrightarrow t_j$. We can also confirm that these correlation functions satisfy the boundary conditions, $\lim_{t_3 \rightarrow t_2} C_3(t_1, t_2, t_3) = C_2(t_1, t_2)$ and $\lim_{t_4 \rightarrow t_3} C_4(t_1, t_2, t_3, t_4) = C_3(t_1, t_2, t_3)$.

The OTOC function (1) for $W = V = n^c$ can be expressed as

$$\begin{aligned}
C(t) &= -C_4(t_+, 0_c, t_-, 0_-) - C_4(0_+, t_+, 0_c, t_-) \\
&\quad + C_3(t_+, 0_c, t_-) + C_3(0_+, t_+, 0_c), \tag{11}
\end{aligned}$$

where $t_{\pm}, 0_{\pm}, 0_c$ are the time points on \tilde{C} defined in Fig. 1 (we can also calculate the OTOC function for $W = c, V = c^{\dagger}$ [52]). Let us emphasize that the result (11) is valid not only in equilibrium but also out of equilibrium. For details of the numerical implementation, we refer to Ref. [34].

The results for the OTOC function $C(t) = -\langle [n^c(t), n^c(0)]^2 \rangle$ are shown in Fig. 2 (red curves) for several U and β . As a comparison, we also plot the dynamical charge susceptibility $\chi(t) \equiv \chi(t, 0)$ [Eq. (8)] (blue), which is a usual response function obeying causality. Both $C(t)$ and $\chi(t)$ grow after $t = 0$, peak out within $t \lesssim 1$, and gradually decay to zero. By definition, $C(t) \geq 0$, while $\chi(t)$ oscillates around zero. Initially the correlations build up as $C(t) \propto t^2$ and $\chi(t) \propto t$. Both of them show a long-time asymptotic behavior $\sim t^{-3}$, reflecting the power-law decay of the Green's function, $R_{\alpha}^R(t, 0) \sim t^{-3/2}$ [52].

In the SYK model or other systems that show the AdS/CFT correspondence, one finds a separation of the relevant time scales; the time scale of the change of $C(t)$ (scrambling time) is longer than that of ordinary response functions such as $\chi(t)$ (thermalization time) by a factor of $\log N$ [9], where N is the number of sites for the SYK model or the number of colors in CFTs. In contrast, there is no clear separation of the two time

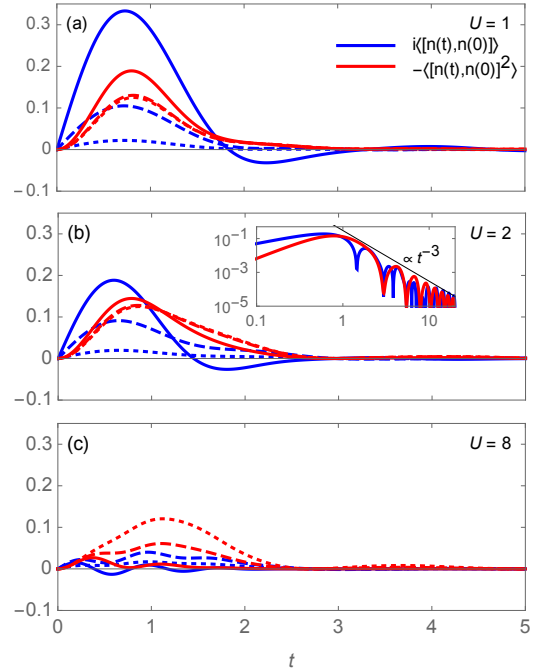


FIG. 2. Dynamical charge susceptibility $\chi(t)$ (blue curves) and out-of-time-ordered charge correlation function $C(t)$ (red) for the FK model with $U = 1$ (a), $U = 2$ (b), and $U = 8$ (c). The solid, dashed, and dotted curves correspond to $\beta = 10, 0.5$, and 0.1 , respectively. The inset shows the corresponding log-log plot for the absolute values, compared with the asymptotic behavior $\propto t^{-3}$.

scales in the FK model (Fig. 2), indicating that the AdS/CFT correspondence cannot be applied here. Given this circumstance, we do not clearly see an exponential growth (butterfly effect) of the deviation of the OTOC from the initial value. In this sense, the FK model does not describe a chaotic system, which is consistent with the expectation that systems with infinitely many conserved charges are not chaotic (and do not thermalize [39]).

Nevertheless, if we look at the temperature dependence of $C(t)$ in Fig. 2, it is very different from that of the ordinary response function $\chi(t)$. As the temperature increases, the amplitude of $\chi(t)$ vanishes irrespective of U , whereas $C(t)$ is enhanced in the insulating phase [$U > 2$, Fig. 2(c)], more or less unchanged at the critical point [$U = 2$, Fig. 2(b)], and suppressed in the metallic phase [$U < 2$, Fig. 2(a)]. In particular, $C(t)$ remains nonvanishing and interaction-dependent in the high-temperature limit, even though the dynamical charge correlations are completely suppressed ($\chi(t) \rightarrow 0$).

To quantify the temperature and interaction dependence of the OTOC at low energy, we compute the OTOC spectral function $C(\omega) = \int_0^{\infty} dt e^{i\omega t} C(t)$ and the dynamical charge susceptibility spectrum $\chi(\omega) = \int_0^{\infty} dt e^{i\omega t} \chi(t, 0)$. $C(\omega = 0)$ measures how much the OTOC grows during the entire dynamics. Figure 3 plots $\chi(\omega = 0)$ and $C(\omega = 0)$ for several U and β . $\chi(\omega = 0)$ monotonically decreases as a function of

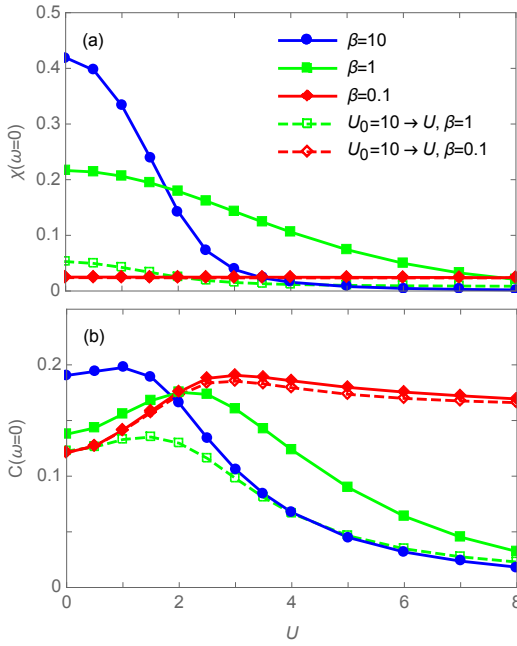


FIG. 3. Comparison between the dynamical charge susceptibility $\chi(\omega)$ (a) and the OTOC spectral function $C(\omega)$ (b) at $\omega = 0$ for the FK model. The dashed curves correspond to interaction quenches $U_0 = 10 \rightarrow U$ with initial temperatures $\beta = 1$ and 0.1 .

U at arbitrary fixed temperature. At sufficiently low temperature, the charge gap opens in the insulating phase ($U > 2$), where $\chi(\omega = 0)$ vanishes. As the temperature increases, thermal excitations take place above the charge gap, leading to an increase in $\chi(\omega = 0)$ in the insulating phase. If the temperature further increases, charge correlations disappear and $\chi(\omega)$ approaches zero. In contrast, $C(\omega = 0)$ is a non-monotonic function of U ; It reaches the maximum at some intermediate coupling ($1 \lesssim U \lesssim 3$) around the metal-insulator transition point [Fig. 3(b)], and decays to zero in the $U \rightarrow \infty$ limit. In particular, the high-temperature limit of $C(\omega = 0)$, which is close to that of $\beta = 0.1$ in Fig. 3(b), shows a highly non-trivial non-zero spectral weight amplified in the insulating phase, whereas the ordinary response function becomes trivial. The overall temperature dependence of $C(\omega = 0)$ is similar to that of $C(t)$ discussed in the preceding paragraph.

Finally, let us discuss how to experimentally measure the OTOC $C(t)$ in many fermion systems. We consider ultracold atomic systems in an optical lattice. There have been several proposals on the measurement of OTOCs. One strategy is to take an interferometric approach with a qubit control [10–13]. Another approach is a time-reversal protocol [20, 21]. Since ultracold atomic systems offer full control over the Hamiltonian parameters with negligible dissipation on the time scale of interest, we propose, based on the latter approach, a serial protocol (Fig. 4) implemented along the contour in Fig. 1(b) that is feasible with available experimental techniques for atomic gases.

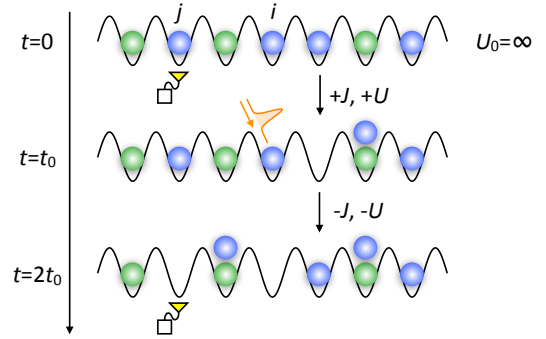


FIG. 4. Illustration of the proposed measurement protocol of the OTOC in ultracold atomic systems with two fermionic species (blue and green). At $t = t_0$, a local pulse is applied to site i , and at $t = 0$ and $t = 2t_0$ the particle density is measured at site j .

We prepare a Mott insulating state with the initial $U_0 = \infty$ tuned by a Feshbach resonance, and measure the number ($\equiv N_1$) of c particles at site j nondestructively. (Note that the Mott insulator is an eigenstate of the particle density.) Then we quench the interaction $U_0 = \infty \rightarrow U$ at $t = 0$, and let the system time-evolve for a duration of t_0 . At $t = t_0$, we apply an instantaneous local potential pulse $\delta H(t) = \varepsilon \delta(t - t_0) n_i^c(t)$ by using a focused laser to shift the energy level of site i [56]. After that, we change the hopping $J_{ij} \rightarrow -J_{ij}$ by shaking the lattice periodically [41], or applying a π pulse [57], or using a Raman process [58] to induce a π phase shift in the kinetic term [59]. At the same time, we quench the interaction $U \rightarrow -U$. With these, we can flip the sign of the Hamiltonian, $H \rightarrow -H$ [60], which enables the system to effectively propagate backward in time (similar to a Loschmidt-echo experiment). After letting the system evolve for another t_0 , we measure the c particle density ($\equiv N_2$) at site j . We repeat this procedure to measure the expectation value of $2N_1N_2 - N_2$ [61]. If we expand it with respect to ε , we obtain

$$\begin{aligned} & \langle 2N_1N_2 - N_2 \rangle \\ &= \text{Tr}[\rho(0)\mathcal{U}(-t_0)e^{i\varepsilon n_i^c}\mathcal{U}(t_0)n_j^c\mathcal{U}(-t_0)e^{-i\varepsilon n_i^c}\mathcal{U}(t_0)(2n_j^c - 1)] \\ &= \langle n_j^c(0) \rangle + \varepsilon^2 \langle [n_i^c(t_0), n_j^c(0)]^2 \rangle + O(\varepsilon^3), \end{aligned} \quad (12)$$

where $\rho(0)$ is the initial density matrix, and $\mathcal{U}(t, t') \equiv \mathcal{U}(t - t')$. The leading-order contribution is exactly the OTOC $C(t)$ for the nonequilibrium system subject to the interaction quench $U_0 \rightarrow U$. In Fig. 3 (dashed curves), we show $\chi(\omega = 0)$ and $C(\omega = 0)$ for the interaction quench where the initial interaction is chosen to be large but finite ($U_0 = 10$). We can see the non-monotonic behavior and characteristic temperature dependence of $C(\omega = 0)$, similar to the results obtained in equilibrium. This scheme is applicable not only to the FK model but also to the Hubbard model. To realize the FK model in ultracold atomic systems, we need a mass imbalance between two fermionic species.

To summarize, we have obtained an exact solution for the OTOCs of the FK model in the thermodynamic limit by gener-

alizing the nonequilibrium DMFT to the extended Kadanoff-Baym contour \tilde{C} . We find that the OTOC $C(t)$ is most enhanced around the metal-insulator transition point, and remains nontrivial in the high-temperature limit, which can be measured in ultracold atomic systems. Our work is a first step toward an analysis of OTOCs in more complicated fermionic lattice models such as the Hubbard model. It is of interest to investigate whether those models, especially in the “strange-metal” phase, show a chaotic behavior, and if so how fast they are scrambled.

We thank I. Danshita, T. Fukuhara, and I. Nakamura for stimulating discussions. NT is supported by JSPS KAKENHI Grant No. JP16K17729. PW acknowledges support from ERC starting grant No. 278023. MU acknowledges support by KAKENHI Grant No. JP26287088 and KAKENHI Grant No. JP15H05855.

-
- [1] P. Hayden and J. Preskill, *J. High Energy Phys.* 09 (2007) 120.
[2] Y. Sekino and L. Susskind, *J. High Energy Phys.* 10 (2008) 065.
[3] S. H. Shenker and D. Stanford, *J. High Energy Phys.* 03 (2014) 067.
[4] S. H. Shenker and D. Stanford, *J. High Energy Phys.* 12 (2014) 046.
[5] A. Kitaev, talk given at Fundamental Physics Prize Symposium Nov. 10, 2014.
[6] A. Kitaev, talks at KITP (2015): <http://online.kitp.ucsb.edu/online/entangled15/kitaev/>, <http://online.kitp.ucsb.edu/online/entangled15/kitaev2/>.
[7] S. H. Shenker and D. Stanford, *J. High Energy Phys.* 05 (2015) 132.
[8] P. Hosur, X.-L. Qi, D. A. Roberts, and B. Yoshida, *J. High Energy Phys.* 02 (2016) 004.
[9] J. Maldacena, S. H. Shenker, and D. Stanford, *J. High Energy Phys.* 08 (2016) 106.
[10] B. Swingle, G. Bentsen, M. Schleier-Smith, and P. Hayden, arXiv:1602.06271.
[11] I. Danshita, M. Hanada, and M. Tezuka, arXiv:1606.02454.
[12] G. Zhu, M. Hafezi, and T. Grover, arXiv:1607.00079.
[13] N. Y. Yao, F. Grusdt, B. Swingle, M. D. Lukin, D. M. Stamper-Kurn, J. E. Moore, and E. Demler, arXiv:1607.01801.
[14] Y. Huang, Y.-L. Zhang, and X. Chen, arXiv:1608.01091.
[15] R. Fan, P. Zhang, H. Shen, and H. Zhai, arXiv:1608.01914.
[16] H. Shen, P. Zhang, R. Fan, and H. Zhai, arXiv:1608.02438.
[17] Y. Chen, arXiv:1608.02765.
[18] B. Swingle and D. Chowdhury, arXiv:1608.03280.
[19] R.-Q. He and Z.-Y. Lu, arXiv:1608.03586.
[20] M. Gärttner, J. G. Bohnet, A. Safavi-Naini, M. L. Wall, J. J. Bollinger, and A. M. Rey, arXiv:1608.08938.
[21] J. Li, R. Fan, H. Wang, B. Ye, B. Zeng, H. Zhai, X. Peng, and J. Du, arXiv:1609.01246.
[22] I. L. Aleiner, L. Faoro, and L. B. Ioffe, arXiv:1609.01251.
[23] A. I. Larkin and Y. N. Ovchinnikov, *Sov. Phys. JETP* **28**, 1200 (1969).
[24] S. Sachdev and J. Ye, *Phys. Rev. Lett.* **70**, 3339 (1993).
[25] S. Sachdev, *Phys. Rev. X* **5**, 041025 (2015).
[26] K. Jensen, *Phys. Rev. Lett.* **117**, 111601 (2016).
[27] J. Polchinski and V. Rosenhaus, *J. High Energy Phys.* 04 (2016) 001.
[28] J. Maldacena and D. Stanford, arXiv:1604.07818.
[29] J. Schwinger, *J. Math. Phys.* **2**, 407 (1961).
[30] L. V. Keldysh, *Sov. Phys. JETP* **20**, 1018 (1965).
[31] L. P. Kadanoff and G. Baym, *Quantum Statistical Mechanics* (W. A. Benjamin, New York, 1962).
[32] P. N. Butcher and D. Cotter, *The Elements of Nonlinear Optics* (Cambridge University Press, Cambridge, England, 1998).
[33] J. K. Freericks, V. M. Turkowski, and V. Zlatić, *Phys. Rev. Lett.* **97**, 266408 (2006).
[34] H. Aoki, N. Tsuji, M. Eckstein, M. Kollar, T. Oka, and P. Werner, *Rev. Mod. Phys.* **86**, 779 (2014).
[35] L. M. Falicov and J. C. Kimball, *Phys. Rev. Lett.* **22**, 997 (1969).
[36] J. K. Freericks and V. Zlatić, *Rev. Mod. Phys.* **75**, 1333 (2003).
[37] A. E. Antipov, Y. Javanmard, P. Ribeiro, and S. Kirchner, *Phys. Rev. Lett.* **117**, 146601 (2016).
[38] J. K. Freericks, *Phys. Rev. B* **77**, 075109 (2008).
[39] M. Eckstein and M. Kollar, *Phys. Rev. Lett.* **100**, 120404 (2008).
[40] N. Tsuji, T. Oka, and H. Aoki, *Phys. Rev. B* **78**, 235124 (2008).
[41] N. Tsuji, T. Oka, and H. Aoki, *Phys. Rev. Lett.* **103**, 047403 (2009).
[42] E. Canovi, P. Werner, and M. Eckstein, *Phys. Rev. Lett.* **113**, 265702 (2014).
[43] A. J. Herrmann, N. Tsuji, M. Eckstein, and P. Werner, arXiv:1609.04708.
[44] A similar set-up has been used in Refs. 9 and 22.
[45] W. Metzner and D. Vollhardt, *Phys. Rev. Lett.* **62**, 324 (1989).
[46] U. Brandt and C. Mielsch, *Z. Phys. B* **75**, 365 (1989).
[47] U. Brandt and C. Mielsch, *Z. Phys. B* **79**, 295 (1990).
[48] U. Brandt and C. Mielsch, *Z. Phys. B* **82**, 37 (1991).
[49] A. Georges, G. Kotliar, W. Krauth, and M. J. Rozenberg, *Rev. Mod. Phys.* **68**, 13 (1996).
[50] The generalized contour delta function on \tilde{C} is defined by $\int_{\tilde{C}} d\tilde{t} \delta_{\tilde{C}}(t, \tilde{t}) g(\tilde{t}) = g(t)$ for an arbitrary contour function $g(t)$.
[51] One can also derive the same result by introducing an external field that couples to the c particle density and taking a functional derivative of the density with respect to the field.
[52] See Supplementary Material.
[53] A. M. Shvaika, *Physica C* **341-348**, 177 (2000).
[54] A. M. Shvaika, *J. Phys. Stud.* **5**, 349 (2001).
[55] J. K. Freericks and P. Miller, *Phys. Rev. B* **62**, 10022 (2000).
[56] In reality, the local pulse will not be perfectly delta-function like. If one uses a pulse shape $f(t, \mathbf{r})$ with finite widths in time and space, we obtain the sum of contributions $\int dt' \int d\mathbf{r}' f(t - t', \mathbf{r}_i - \mathbf{r}') \langle [n_{\mathbf{r}'}^c(t'), n_j^c(0)]^2 \rangle$.
[57] N. Tsuji, T. Oka, H. Aoki, and P. Werner, *Phys. Rev. B* **85**, 155124 (2012).
[58] D. Jaksch and P. Zoller, *Ann. Phys.* **315**, 52 (2005).
[59] During the sign reversal of the hopping, there might occur heating. In this respect, the π pulse method is superior to others since the system is driven only in a short time interval.
[60] If one uses a periodic drive, one has to quench $U \rightarrow -|J_0(A)|U$ [$J_0(A)$ is the zeroth-order Bessel function and A is the amplitude of the drive] so that the ratio between the hopping and interaction remains unchanged. In this case, the time after $t = t_0$ should be rescaled accordingly.
[61] Since $N_1, N_2 = 0, 1$ for fermionic systems, it is enough to measure the parity of the particle density.

Supplementary Material for “Exact Out-of-Time-Ordered Correlation Functions for an Interacting Lattice Fermion Model”

Naoto Tsuji,¹ Philipp Werner,² and Masahito Ueda^{1,3}

¹RIKEN Center for Emergent Matter Science (CEMS), Wako 351-0198, Japan

²Department of Physics, University of Fribourg, 1700 Fribourg, Switzerland

³Department of Physics, University of Tokyo, Hongo, Tokyo 113-0033, Japan

I. EQUIVALENCE OF THE LOCAL AND LATTICE SUSCEPTIBILITIES AT GENERAL MOMENTUM

In this section, we explicitly show that the local dynamical charge susceptibility (8) of the Falicov-Kimball (FK) model, calculated from Eq. (7), is equal to the previously known result for the lattice dynamical charge susceptibility at general momentum [1, 2].

To see this, we substitute Eq. (7) in Eq. (8) to obtain

$$\chi(t, t') = i\theta(t - t') \sum_{\alpha} w_{\alpha} [R_{\alpha}^{>}(t, t') R_{\alpha}^{<}(t', t) - R_{\alpha}^{<}(t, t') R_{\alpha}^{>}(t', t)]. \quad (\text{S.1})$$

We replace the greater Green's functions with the lesser, retarded, and advanced components by using the relations

$$\theta(t - t') R_{\alpha}^{>}(t, t') = \theta(t - t') R_{\alpha}^{<}(t, t') + R_{\alpha}^R(t, t'), \quad (\text{S.2})$$

$$\theta(t - t') R_{\alpha}^{>}(t', t) = \theta(t - t') R_{\alpha}^{<}(t', t) - R_{\alpha}^A(t', t). \quad (\text{S.3})$$

This results in the expression

$$\chi(t, t') = i \sum_{\alpha} w_{\alpha} [R_{\alpha}^R(t, t') R_{\alpha}^{<}(t', t) + R_{\alpha}^{<}(t, t') R_{\alpha}^A(t', t)], \quad (\text{S.4})$$

or, in the Fourier transformed form,

$$\chi(\omega) = i \int \frac{d\omega'}{2\pi} \sum_{\alpha} w_{\alpha} [R_{\alpha}^R(\omega + \omega') R_{\alpha}^{<}(\omega') + R_{\alpha}^{<}(\omega + \omega') R_{\alpha}^A(\omega')]. \quad (\text{S.5})$$

By means of the fluctuation-dissipation relation $R_{\alpha}^{<}(\omega) = f(\omega)[R_{\alpha}^A(\omega) - R_{\alpha}^R(\omega)]$ [$f(\omega) = 1/(e^{\beta\omega} + 1)$ is the Fermi distribution function], Eq. (S.5) can be written as

$$\begin{aligned} \chi(\omega) = & -i \int \frac{d\omega'}{2\pi} \sum_{\alpha} w_{\alpha} \left\{ f(\omega') R_{\alpha}^R(\omega + \omega') R_{\alpha}^R(\omega') \right. \\ & - f(\omega + \omega') R_{\alpha}^A(\omega + \omega') R_{\alpha}^A(\omega') \\ & \left. - [f(\omega') - f(\omega + \omega')] R_{\alpha}^R(\omega + \omega') R_{\alpha}^A(\omega') \right\}. \quad (\text{S.6}) \end{aligned}$$

Let us recall that the configuration-dependent Green's function $R_{\alpha}(t, t')$ is in a nontrivial way related to the local Green's function and the self-energy [1],

$$\frac{1}{G^X(\omega)G^Y(\omega')} - \frac{1}{\sum_{\alpha} w_{\alpha} R_{\alpha}^X(\omega)R_{\alpha}^Y(\omega')} = \frac{\Sigma^X(\omega) - \Sigma^Y(\omega')}{G^X(\omega) - G^Y(\omega')}, \quad (\text{S.7})$$

where $X, Y = R, A$. The right-hand side of Eq. (S.7) is the irreducible dynamical charge vertex function. The relation (S.7) can be proven as follows:

$$\begin{aligned} \sum_{\alpha} w_{\alpha} R_{\alpha}^X(\omega)R_{\alpha}^Y(\omega') &= \sum_{\alpha} w_{\alpha} \frac{R_{\alpha}^X(\omega) - R_{\alpha}^Y(\omega')}{R_{\alpha}^{Y-1}(\omega') - R_{\alpha}^{X-1}(\omega)} \\ &= \frac{\sum_{\alpha} w_{\alpha} [R_{\alpha}^X(\omega) - R_{\alpha}^Y(\omega')]}{R_0^{Y-1}(\omega') - R_0^{X-1}(\omega)} \\ &= \frac{G^X(\omega) - G^Y(\omega')}{[G^{Y-1}(\omega') + \Sigma^Y(\omega')] - [G^{X-1}(\omega) + \Sigma^X(\omega)]}. \quad (\text{S.8}) \end{aligned}$$

In deriving the second equality, we used $R_1^{X-1}(\omega) = R_0^{X-1}(\omega) - U$. In deriving the last equality, we used the impurity solution (4) and the impurity Dyson equation $G^X(\omega) = [R_0^{X-1}(\omega) - \Sigma^X(\omega)]^{-1}$ [note that $R_0^X(\omega)$ is the Weiss Green's function]. One immediately gets Eq. (S.7) from the last line of Eq. (S.8). Substituting Eq. (S.7) into Eq. (S.6), we arrive at

$$\begin{aligned} \chi(\omega) = & -i \int \frac{d\omega'}{2\pi} \left\{ f(\omega') \frac{G^R(\omega + \omega')G^R(\omega')}{1 - G^R(\omega + \omega')G^R(\omega') \frac{\Sigma^R(\omega + \omega') - \Sigma^R(\omega')}{G^R(\omega + \omega') - G^R(\omega')}} \right. \\ & - f(\omega + \omega') \frac{G^A(\omega + \omega')G^A(\omega')}{1 - G^A(\omega + \omega')G^A(\omega') \frac{\Sigma^A(\omega + \omega') - \Sigma^A(\omega')}{G^A(\omega + \omega') - G^A(\omega')}} \\ & \left. - [f(\omega') - f(\omega + \omega')] \frac{G^R(\omega + \omega')G^A(\omega')}{1 - G^R(\omega + \omega')G^A(\omega') \frac{\Sigma^R(\omega + \omega') - \Sigma^A(\omega')}{G^R(\omega + \omega') - G^A(\omega')}} \right\}. \quad (\text{S.9}) \end{aligned}$$

This is nothing but the lattice dynamical charge susceptibility of the FK model at general momentum [1, 2] [for the hypercubic lattice the general momentum corresponds to $X(\mathbf{q}) = \lim_{d \rightarrow \infty} \sum_{i=1}^d \cos q_i/d = 0$ [2, 3]]. The difference of the sign is due to the different definitions of the charge susceptibility. The physical reason for the coincidence between the local and lattice susceptibilities is explained in the main text.

II. LONG-TIME ASYMPTOTIC BEHAVIOR OF THE OUT-OF-TIME-ORDERED CORRELATION FUNCTION

In this section, we explain the long-time asymptotic form of the out-of-time-ordered correlation function $C(t) = -\langle [n^c(t), n^c(0)]^2 \rangle$ for the FK model.

Here $C(t)$ is determined from Eqs. (9), (10), and (11) in the main text. We note that $C(t)$ is obtained as a sum of products of $R_{\alpha}(t, t')$. Since $R_{\alpha}(t, t')$ is a 2-point function, any $R_{\alpha}(t, t')$ with $t, t' \in \bar{\mathcal{C}}$ reduces to $R_{\alpha}(t, t')$ with $t, t' \in \mathcal{C}$. For example,

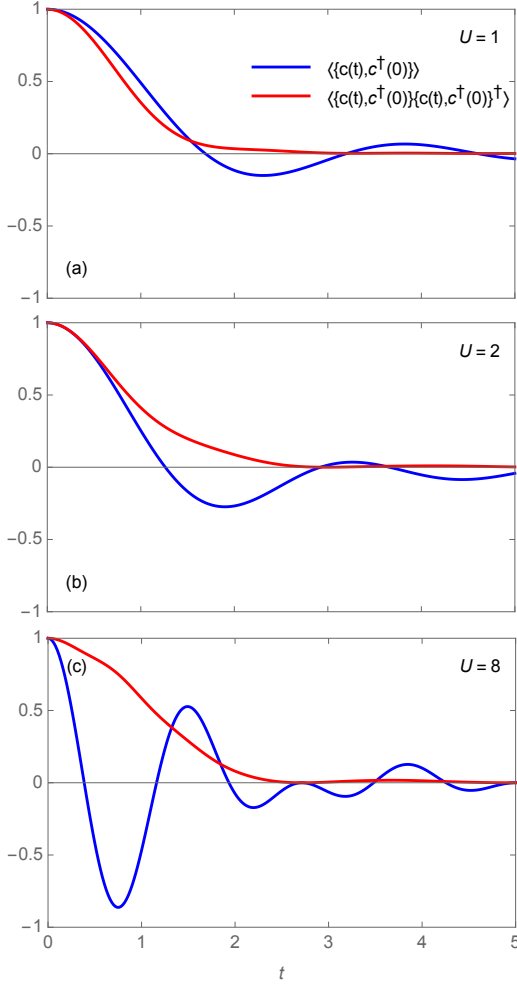


FIG. 1. Comparison between the retarded Green's function ($\times i$) $\langle\langle c(t), c^\dagger(0) \rangle\rangle$ (blue curves) and the out-of-time-ordered correlation function $\langle\langle c(t), c^\dagger(0) \rangle\rangle \langle\langle c(t), c^\dagger(0) \rangle\rangle^\dagger$ (red) for the FK model with $U = 1$ (a), $U = 2$ (b), and $U = 8$ (c). These functions do not depend on temperature.

$R_\alpha(t_+, 0_c) = R_\alpha^>(t, 0)$ and $R_\alpha(t_-, 0_c) = R_\alpha^<(t, 0)$. Thus $C(t)$ can be expressed as a contour function defined on the conventional Kadanoff-Baym contour \mathcal{C} . The result is

$$C(t) = \sum_\alpha w_\alpha |R_\alpha^R(t, 0)|^2 \left[|R_\alpha^>(t, 0)|^2 + |R_\alpha^<(t, 0)|^2 - |R_\alpha^R(t, 0)|^2 + 2R_\alpha^<(t, t)R_\alpha^<(0, 0) - iR_\alpha^<(t, t) - iR_\alpha^<(0, 0) \right]. \quad (\text{S.10})$$

The long-time behavior of $|R_\alpha^{R, \gtrless}(t, 0)|$ is determined by the branch points in $R_\alpha^{R, \gtrless}(\omega)$ at the spectral edges ($\omega = \omega_c$), i.e., $R_\alpha^{R, \gtrless}(\omega) \sim (\text{regular part}) + (\text{const.}) \times \sqrt{\omega^2 - \omega_c^2}$ ($\omega \sim \omega_c$). By the saddle point approximation, one finds that $|R_\alpha^{R, \gtrless}(t, 0)| \sim t^{-3/2}$ in the long-time limit both in the metallic and insulating phases (although the number of branch points changes at the phase transition point). This is also confirmed numerically. [If one takes a lattice other than the Bethe lattice, the asymptotic

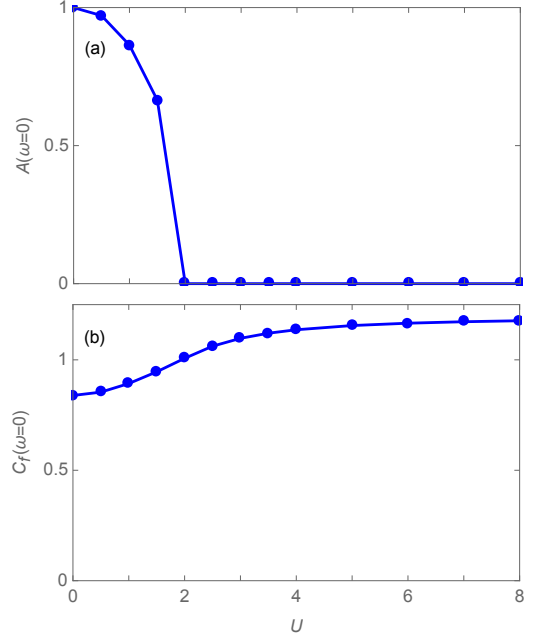


FIG. 2. Single-particle $[A(\omega)$ (a)] and OTOC $[C_f(\omega)$ (b)] spectral functions for the FK model at zero frequency. These functions do not depend on temperature.

behavior may change according to the form of $R_\alpha^{R, \gtrless}(\omega)$ at the spectral edges.]

Since $R_\alpha^<(t, t)$ approaches a constant for $t \rightarrow \infty$, the long-time behavior of $C(t)$ is governed by $|R_\alpha^R(t, 0)|^2 \sim t^{-3}$. The terms in the fourth power of R_α in Eq. (S.10) give subleading contributions to the long-time behavior.

III. FERMIONIC OUT-OF-TIME-ORDERED CORRELATION FUNCTION

In this section, we show the results for the out-of-time-ordered correlation function constructed from the fermionic operators $V = c_i^\dagger, W = c_i$. A natural extension of the definition of the OTOC (1) to fermionic operators is given by $\langle\langle \{W(t), V(0)\} \{W(t), V(0)\}^\dagger \rangle\rangle$, where we have replaced the commutator in Eq. (1) with an anticommutator. This fermionic OTOC can be evaluated exactly for the infinite-dimensional FK model with the same technique as explained in the main text:

$$\begin{aligned} C_f(t) &\equiv \langle\langle \{c(t), c^\dagger(0)\} \{c(t), c^\dagger(0)\}^\dagger \rangle\rangle \\ &= \sum_\alpha w_\alpha [R_\alpha^>(t, 0) - R_\alpha^<(t, 0)] [R_\alpha^<(0, t) - R_\alpha^>(0, t)] \\ &= \sum_\alpha w_\alpha |R_\alpha^R(t, 0)|^2. \end{aligned} \quad (\text{S.11})$$

It satisfies $C_f(t) \geq 0$.

In Fig. 1, we compare the retarded Green's function $iG^R(t, 0)$ and $C_f(t)$ for several U . We note that both $G^R(t, 0)$

and $C_f(t)$ are independent of the system's temperature, since the retarded components of Green's functions and the self-energy form a closed set of self-consistent equations in the case of the FK model, and can be determined independently of the Matsubara components. As one can see in Fig. 1, the timescale on which $C_f(t)$ changes is comparable to that of $G^R(t, 0)$ (and the dynamical charge correlation function). The initial drop of $C_f(t)$ is delayed compared with $G^R(t, 0)$ in the insulating phase ($U \geq 2$). In the long-time limit, the functions decay as power laws: $iG^R(t, 0) \sim t^{-3/2}$ and $C_f(t) \sim t^{-3}$.

To illustrate the dependence of the OTOC $C_f(t)$ on the interaction U , we define the OTOC spectral function

$$C_f(\omega) = \int_0^\infty dt e^{i\omega t} C_f(t). \quad (\text{S.12})$$

In Fig. 2, we compare $C_f(\omega)$ at $\omega = 0$ with the single-particle

spectral function $A(\omega) = -\frac{1}{\pi} \text{Im} G^R(\omega)$ at $\omega = 0$ for the FK model. In the metallic phase ($U < 2$), there is a nonzero spectral weight at the Fermi energy, while in the insulating phase ($U > 2$) the energy gap opens and the spectral weight vanishes. On the other hand, $C_f(\omega = 0)$ grows as U is increased, and saturates in the strong-coupling limit. This implies that in the insulating phase, even though the single-particle motions are frozen at low energy, the information spreading still occurs to some extent.

-
- [1] J. K. Freericks and P. Miller, Phys. Rev. B **62**, 10022 (2000).
 - [2] J. K. Freericks and V. Zlatić, Rev. Mod. Phys. **75**, 1333 (2003).
 - [3] A. Georges, G. Kotliar, W. Krauth, and M. J. Rozenberg, Rev. Mod. Phys. **68**, 13 (1996).